Arabian Journal of Chemistry (2022) **15**, 104263

King Saud University

Arabian Journal of Chemistry

www.ksu.edu.sa
www.sciencedirect.com

ORIGINAL ARTICLE

Theoretical study of the structure and fundamental properties of AZn_2N_2 (A = Ca, Sr, Ba)

Diwen Liu [a,*], **Huan Peng** [a], **Rongjian Sa** [b,*]

[a] *School of Materials and Chemical Engineering, Pingxiang University, Pingxiang 337055, China*
[b] *College of Materials and Chemical Engineering, Fujian Key Laboratory of Functional Marine Sensing Materials, Minjiang University, Fuzhou 350108, China*

Received 6 July 2022; accepted 11 September 2022
Available online 19 September 2022

KEYWORDS

AZn_2N_2;
Stability;
Elastic constant;
Optoelectronic properties;
DFT

Abstract The structure, stability, elastic, electronic, and optical properties of trigonal AZn_2N_2 (A = Ca, Sr, Ba) are simulated and compared in this work. The stability and physical properties of $BaZn_2N_2$ are mainly highlighted. According to the calculated results, three compounds are thermodynamically and mechanically stable, and they are brittle materials. The stability of trigonal $BaZn_2N_2$ is confirmed by using the different theoretical approaches. The direct band gap transition is allowed at the Γ point for each compound. The predicted direct band gaps are 1.733, 1.507, and 1.510 eV for $CaZn_2N_2$, $SrZn_2N_2$, and $BaZn_2N_2$, respectively. The valence band is mostly composed of the N-2p orbitals, while the conduction band is mainly contributed from the Ca-3d/Sr-4d/Ba-5d orbitals. The results show that the electron shows high mobility for carrier transport, and the value of exciton binding energy is less than 80 meV. Furthermore, compared to $CaZn_2N_2$ and $SrZn_2N_2$, $BaZn_2N_2$ shows excellent light absorption capacity in the visible region. This study indicates that $BaZn_2N_2$ is a desirable material for solar cell applications.

1. Introduction

The most representative nitrides are GaN and its alloys such as $Ga_{1-x}Al_xN$ and $Ga_{1-x}In_xN$ because they are the important materials for optoelectronic devices (Ul Haq et al., 2014; Özdemir et al., 2019). The electronic, optical, and thermoelectric properties of two-dimensional III-nitrides $Ga_{1-x}Al_xN$ and $Ga_{1-x}In_xN$ have been been demonstrated through density functional theory (DFT) calculations (Wines et al., 2020). However, these compounds contain the rare or toxic elements, which is difficult to achieve large-scale commercial applications. Therefore, it is of great importance to explore novel nitrides, which are composed of earth-abundant and non-toxic elements. The fundamental physical properties of II–IV–N_2 nitrides and their alloys have been investigated in recent years, such as $ZnSiN_2$ (Häusler et al., 2017; Mallmann et al., 2019); $ZnGeN_2$ (Häusler et al., 2017; Mallmann et al., 2019); $MgSiN_2$ (Mallmann et al., 2019; Häusler et al., 2018), $MgGeN_2$ (Mallmann et al., 2019; Häusler et al., 2018); $ZnSnN_2$ (Cao et al., 2017; Laidouci et al., 2020; Tsunoda et al., 2018), and $Zn_{1-x}Mg_xSnN_2$ (Yamada et al., 2021).

* Corresponding authors.
E-mail addresses: liudiwen1987@163.com (D. Liu), rjsa@mju.edu.cn (R. Sa).

Peer review under responsibility of King Saud University.

ELSEVIER Production and hosting by Elsevier

https://doi.org/10.1016/j.arabjc.2022.104263

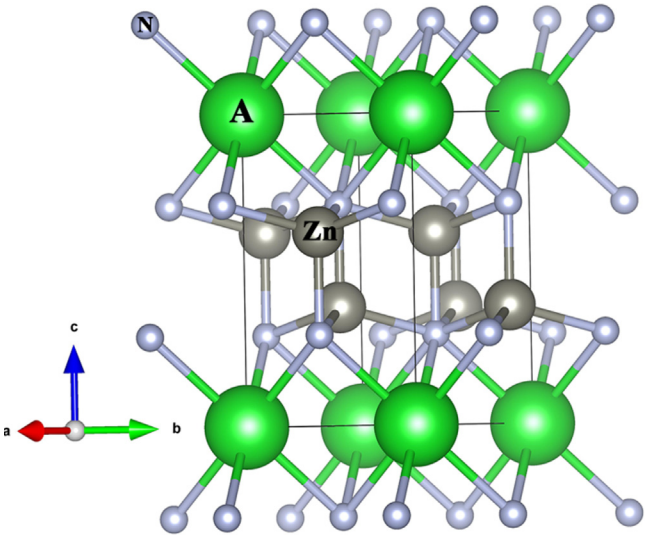

Fig. 1 The trigonal structure of AZn_2N_2 (A = Ca, Sr, Ba).

The computational screening of ternary nitrides is conducted, and some novel compounds are finally identified (Hinuma et al., 2016). For example, $CaZn_2N_2$ can be synthesized by high-pressure methods, and it is a direct band gap semiconductor with 1.8 eV (Hinuma et al., 2016). The band gap energy of $CaZn_2N_2$ is narrowed to 1.6 eV by the substitution of Sr for Ca, which is further confirmed by the recent experiment (Kikuchi et al., 2021). In addition, the direct band gap can be widely tuned from ~ 1.8 to ~ 3.2 eV between $CaZn_2N_2$ and $CaMg_2N_2$ (Tsuji et al., 2019). $CaZn_2N_2$ is a promising candidate for next-generation semiconductor in the filed of light-emitting diodes and solar cells (Tsuji et al., 2019; Huang et al., 2022). A detailed theoretical study is performed to reveal the impact of pressure on the dynamical, elastic, and thermal properties of $CaZn_2N_2$ (Zhao et al., 2017). The structure and fundamental physical properties of $MgBe_2N_2$, $CaBe_2N_2$, $CaMg_2N_2$, $SrMg_2N_2$, $CaZn_2N_2$, and $SrZn_2N_2$ are thoroughly studied via first-principles calculations (Khan et al., 2019; Khan et al., 2018; Khan et al., 2018; Murtaza et al., 2018; Murtaza et al., 2018; Murtaza et al., 2018). It is revealed from our recent theoretical work that the band gaps of $CaZn_2N_2$ and $SrZn_2N_2$ are effectively regulated by the partial substitution of Cd for Zn (Liu et al., 2022).

The structures and physical properties of both $CaZn_2N_2$ and $SrZn_2N_2$ have been reported experimentally and theoretically (Hinuma et al., 2016; Kikuchi et al., 2021; Zhao et al., 2017). However, no available experimental and theoretical reports are conducted for exploring the fundamental properties of $BaZn_2N_2$. Therefore, a comprehensive study is required to investigate the structure, stability, elastic, electronic, and optical properties of $BaZn_2N_2$. Moreover, it is vital to know whether the trigonal phase is stable for $BaZn_2N_2$. The thermodynamic, dynamic, thermal, and mechanical stability of $BaZn_2N_2$ is evaluated for the first time. The elastic, electronic, and optical properties of AZn_2N_2 (A = Ca, Sr, Ba) are compared and discussed in detail. The influence of different cations on the various physical properties of AZn_2N_2 is revealed. The results suggest that $BaZn_2N_2$ is a stable and desirable material for solar cell applications.

Table 2 The atomic coordinates for $BaZn_2N_2$.

Atom	*x*	*y*	*z*
Ba	0.00000	0.00000	0.00000
Zn1	0.33333	0.66667	0.62018
Zn2	0.66667	0.33333	0.37982
N1	0.33333	0.66667	0.29112
N2	0.66667	0.33333	0.70888

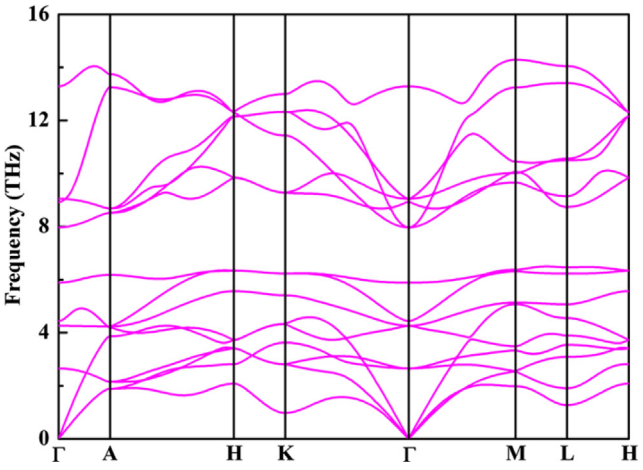

Fig. 2 The phonon spectrum curves of trigonal $BaZn_2N_2$.

2. Computational details

The structure and physical properties of trigonal AZn_2N_2 (A = Ca, Sr, Ba) were simulated in this work by using first-principles calculations as implemented in the Vienna ab initio simulation package (VASP) (Kresse and Furthmüller, 1996). The interaction between icons and valance electrons was dealt by the projector augmented wave (PAW) (Blöchl, 1994) method. The structure was fully relaxed by employing Perdew–Burke–Ernzerhof (PBE) functional within the generalized gradient approximation (GGA) (Perdew et al., 1996). The

Table 1 The various structural parameters for AZn_2N_2 (A = Ca, Sr, Ba).

Compound	$a = b$ (Å)	c (Å)	V (Å^3)	$\alpha = \beta$ (°)	γ (°)	A – N (Å)
$CaZn_2N_2$	3.48	6.04	63.35	90	120	2.54
Exp.[a]	3.46	6.01	/	/	/	/
Theor.[a]	3.45	5.99	/	/	/	/
$SrZn_2N_2$	3.57	6.28	69.47	90	120	2.69
Theor.[b]	3.48	6.15	/	/	/	/
$BaZn_2N_2$	3.66	6.60	76.64	90	120	2.86

[a] Hinuma et al. (2016).
[b] Kikuchi et al. (2021).

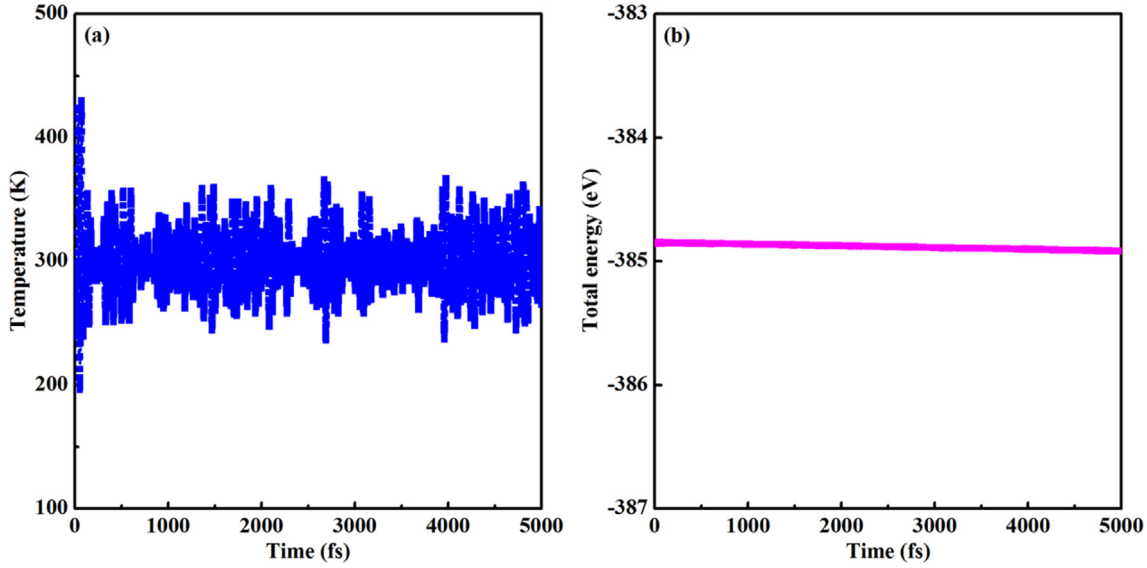

Fig. 3 The variations of (a) temperature and (b) total energy for $BaZn_2N_2$ at the AIMD simulations.

cut-off energy was set to be 520 eV. The *k*-point mesh of 8 × 8 × 4 was adopted for all calculations. The convergence criteria of total energy and the forces on each atom were less than 10^{-6} eV and 10^{-3} eV/Å, respectively. The electronic and optical properties of AZn_2N_2 (A = Ca, Sr, Ba) were obtained by employing the hybrid functional HSE06 (Heyd et al., 2003). A 3 × 3 × 2 supercell was constructed for trigonal $BaZn_2N_2$ in order to calculate the phonon dispersion curves based on the Phonon code (Togo and Tanaka, 2015). Furthermore, ab initio molecular dynamics (AIMD) simulations were performed for trigonal $BaZn_2N_2$ at room temperature (300 K).

3. Results and discussion

3.1. Structural properties and stability

The compound AZn_2N_2 (A = Ca, Sr) crystallizes in the trigonal structure (space group: $P\bar{3}m1$) (Hinuma et al., 2016; Kikuchi et al., 2021), while the trigonal crystal structure is not reported experimentally for $BaZn_2N_2$ so far. Therefore, the trigonal crystal structure of $BaZn_2N_2$ was constructed by substituting Ba for Ca in $CaZn_2N_2$. In addition, the physical properties of both $CaZn_2N_2$ and $SrZn_2N_2$ are presented in order to explore the effect of different cations on the structure and properties of AZn_2N_2. Fig. 1 depicts the trigonal crystal structure of AZn_2N_2 (A = Ca, Sr, Ba). The obtained structural parameters of three compounds are demonstrated in Table 1. The lattice constants of $CaZn_2N_2$ and $SrZn_2N_2$ are consistent with the recent experimental and theoretical data (Hinuma et al., 2016; Kikuchi et al., 2021). The lattice constant and bond length are increased from $CaZn_2N_2$ to $BaZn_2N_2$. The computed lattice constants of $BaZn_2N_2$ are $a = b = 3.66$ Å and $c = 6.60$ Å, respectively. The atomic coordinates in the trigonal structure of $BaZn_2N_2$ are listed in Table 2.

The thermodynamic stability of three compounds is checked by the following formation energy (E_f) formula:

$$E_f = E_{AZn_2N_2} - E_A - 2 \times E_{Zn} - E_{N_2} \quad (1)$$

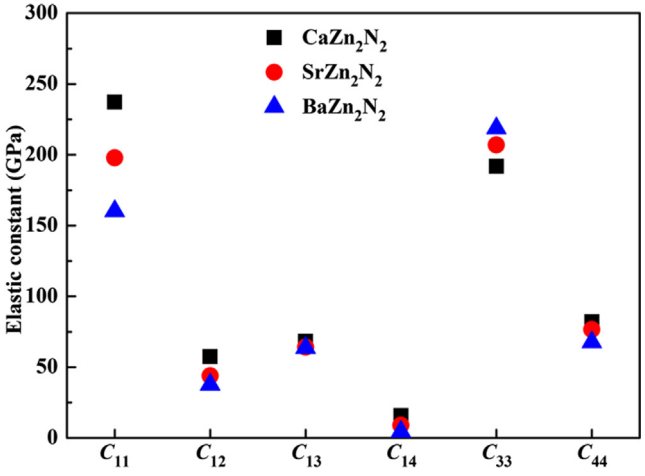

Fig. 4 The trend of six independent elastic constants for $CaZn_2N_2$, $SrZn_2N_2$, and $BaZn_2N_2$.

The calculated values of E_f are −1.94, −1.37, and −0.64 eV/f.u., respectively. The results indicate that three compounds can be synthesized at proper conditions and also confirm their thermodynamic stability. It is well known that the lower the E_f, the better the stability, thus the thermodynamic stability is reduced from $CaZn_2N_2$ to $BaZn_2N_2$. Furthermore, it is vital to assess the dynamical stability of trigonal $BaZn_2N_2$. The computed phonon dispersion curves are illustrated in Fig. 2. It is dynamically stable for trigonal $BaZn_2N_2$ because there is no negative frequency. It is observed that three acoustic phonon frequencies are zero at the Γ point, which ensure the dynamical stability of $BaZn_2N_2$. It is noted for $BaZn_2N_2$ that although the tetragonal structure has a lower total energy (~80 meV/f.u.) than that of the trigonal structure, the tetragonal structure is not dynamically stable because there are many negative frequencies according to the calculations of phonon spectrum. The AIMD simulations are conducted to further verify the thermal stability of $BaZn_2N_2$. As shown in

Fig. 3, it is widely fluctuated for the temperature, but the total energy varies little throughout the whole simulation. The trigonal structure is still maintained, thus the thermal stability is proved.

3.2. Mechanical properties

The elastic properties of $CaZn_2N_2$, $SrZn_2N_2$, and $BaZn_2N_2$ are calculated for the first time. It is widely known that there are six independent elastic constants for a trigonal crystal system. The complete Born stability criteria for a trigonal system is the following four conditions (Mouhat and Coudert, 2014):

$$C_{11} > |C_{12}|, C_{13}^2 < \frac{1}{2}C_{33}(C_{11}+C_{12}), C_{44} > 0, C_{14}^2 < \frac{1}{2}C_{44}(C_{11}-C_{12}) \quad (2)$$

The six elastic constants are displayed in Fig. 4. It is verified that three compounds are mechanically stable since all the mentioned conditions are met. It is apparent that five elastic constants (such as C_{11}, C_{12}, C_{13}, C_{14}, and C_{44}) are decreased from $CaZn_2N_2$ to $BaZn_2N_2$, while the only elastic constant C_{33} is increased. The bulk modulus (B) and the shear modulus (G) can be computed by applying the Voigt–Reuss–Hill approximations (Hill, 1952). The Poisson's ratio (v) is obtained by the formula: $v = (3B - G)/[2(3B + G)]$ (Wu et al., 2007). Two parameters of B/G and v can discern the brittleness or ductility feature of a compound. If the values of B/G and v are less than 1.75 and 0.26, the compound is brittle, otherwise, the ductile behavior is observed (Hadi et al., 2017; Pugh, 1954). The results show that the values of B/G and v are in the range of 1.41–1.49 and 0.21–0.23, respectively. It can be inferred that three compounds are brittle materials in nature.

3.3. Electronic properties

The band structure and transition dipole moment (TDM) in the Brillouin zone of each compound are calculated at the PBE functional. First of all, it can be seen from Fig. 5 that they are direct band gap semiconductors with the valence band maximum (VBM) and conduction band minimum (CBM) at the Γ point. Secondly, the degree of direct electronic transition between the VBM and CBM edges is mainly determined by the value of TDM. According to the previous detailed theoretical study (Meng et al., 2017), there are four types of transitions: (i) all k points forbidden, (ii) partial k points forbidden, (iii) weak transition allowed, and (iv) strong transition allowed. The values of TDM at various k points are illustrated in Fig. 5. It is clear that the allowed and strong transition between the band edges at the Γ point is revealed for the studied three compounds, which is desirable for solar cell applications.

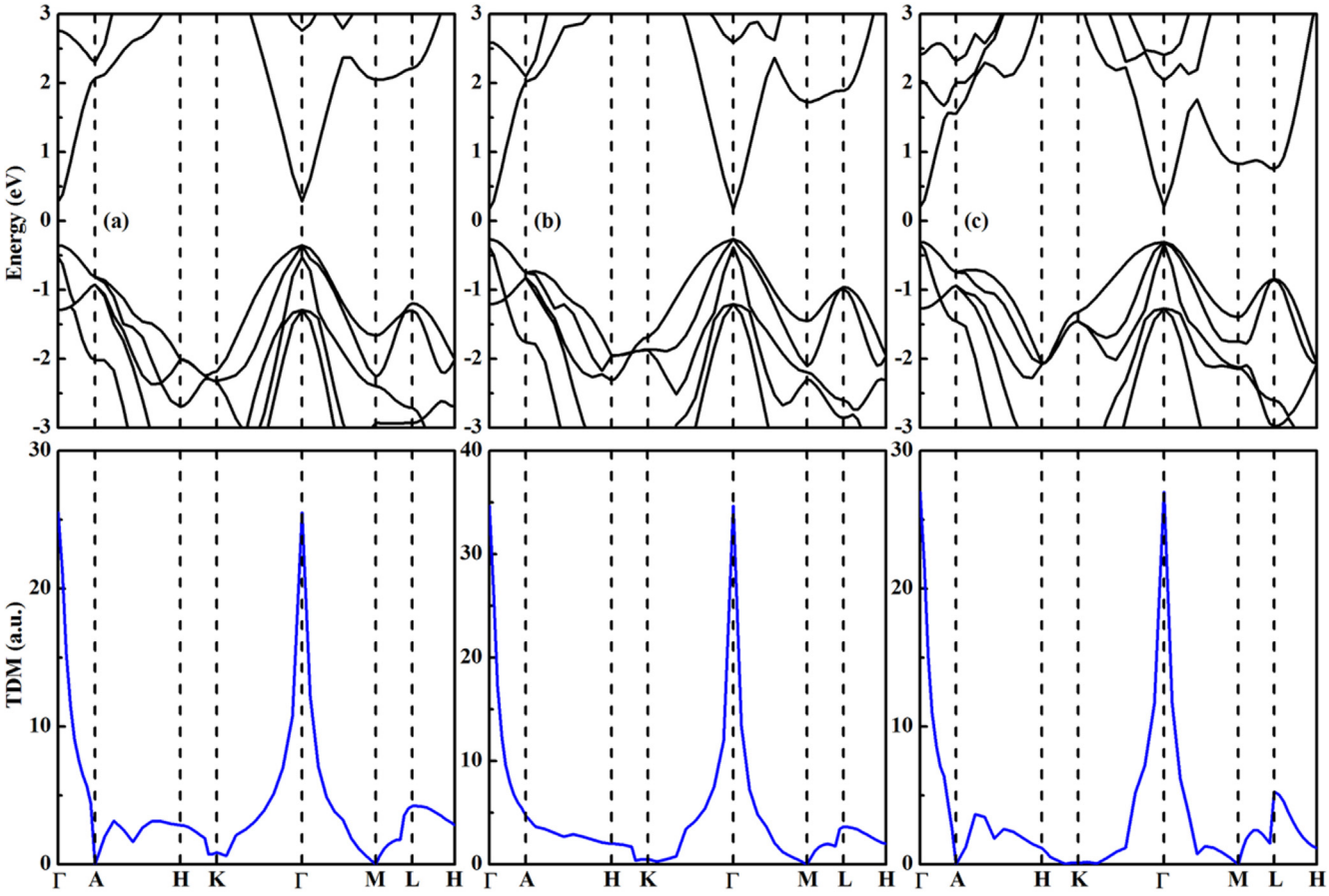

Fig. 5 The band structures (upper) and transition dipole moments (lower) of (a) $CaZn_2N_2$, (b) $SrZn_2N_2$, and (c) $BaZn_2N_2$ at the PBE functional.

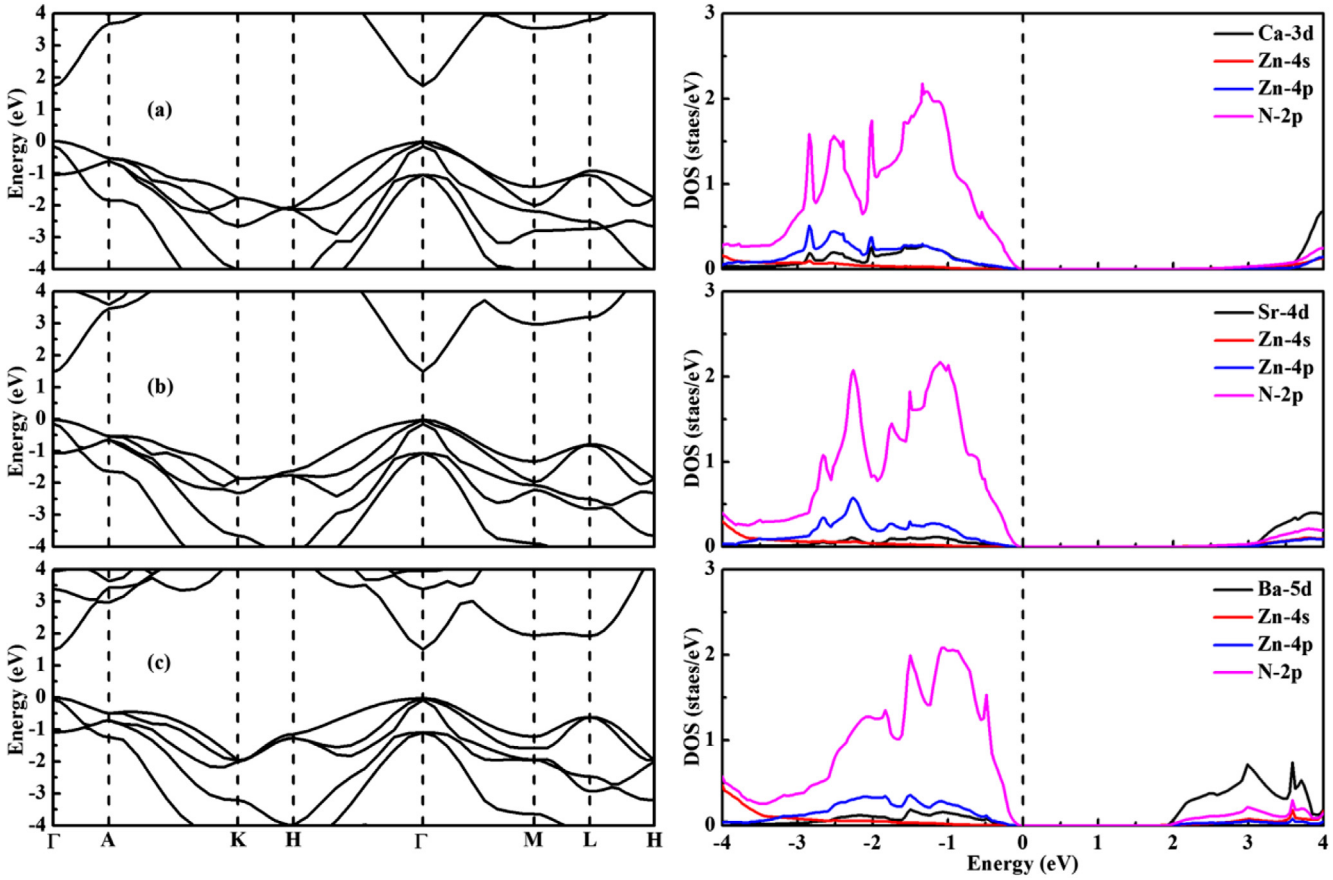

Fig. 6 Band structures (left) and density of states (right) of (a) $CaZn_2N_2$, (b) $SrZn_2N_2$, and (c) $BaZn_2N_2$.

Table 3 The computed values of m_e^*, m_h^*, m_r^*, ε, and E_b for AZn_2N_2 (A = Ca, Sr, Ba).

Compound	m_e^* (m_0)	m_h^* (m_0)	m_r^*	ε	E_b (meV)
$CaZn_2N_2$	0.209	1.374	0.181	5.705	76
$SrZn_2N_2$	0.217	1.345	0.187	5.942	72
$BaZn_2N_2$	0.244	1.317	0.206	6.637	63

The calculated band gaps are 0.637 and 0.442 eV for $CaZn_2N_2$ and $SrZn_2N_2$ when the standard PBE functional is used. The theoretical band gaps of both compounds are seriously underestimated compared to the experimental values (Kikuchi et al., 2021; Tsuji et al., 2019). The corrected band gaps calculated from the HSE06 functional are 1.733 and 1.507 eV for $CaZn_2N_2$ and $SrZn_2N_2$, which are reasonable consistent with the recent experimental data (1.8 eV for $CaZn_2N_2$ and 1.6 eV for $SrZn_2N_2$) (Kikuchi et al., 2021; Tsuji et al., 2019). It is concluded that the lower band gap can be realized for AZn_2N_2 by varying the earth-alkali metal element. It is observed from Fig. 6 that $BaZn_2N_2$ is also a direct band gap compound at the Γ point. It is interesting that the direct band gap is 1.510 eV for $BaZn_2N_2$. It is noted that the band gap difference between $SrZn_2N_2$ and $BaZn_2N_2$ is negligible. By analyzing the density of states of three compounds, it is disclosed that the VBM is largely contributed from the N-2p orbitals, while the CBM is dominated by the contribution from the Ca-3d/Sr-4d/Ba-5d orbitals. The contributions from the Zn-4 s and Zn-4p orbitals are little for the edges of VBM and CBM.

The mobility of the carriers is a crucial index for optoelectronic applications. The effective masses of electron (m_e^*) and hole (m_h^*) can be derived from the curvatures around the VBM and CBM with the following relation (Green, 1990):

$$m^* = \hbar^2\left[\frac{\partial^2\varepsilon(k)}{\partial k^2}\right]^{-1} \quad (3)$$

where ħ and $\varepsilon(k)$ are the reduced Planck constant and orbit eigenvalue, respectively. In addition, the exciton binding energy (E_b) can be further obtained by the following equation (Liu et al., 2021):

$$E_b \approx \frac{13.56m_r^*}{m_0\varepsilon^2} \quad (4)$$

where m_r^*, m_0, and ε are the reduced effective mass ($m_r^* = m_e^* \times m_h^*/(m_e^* + m_h^*)$), static electron mass, and static dielectric constant, respectively. The effective masses of electron (m_e^*) and hole (m_h^*) along with the Γ→A direction are computed for AZn_2N_2 (A = Ca, Sr, Ba). It can be seen from Table 3 that

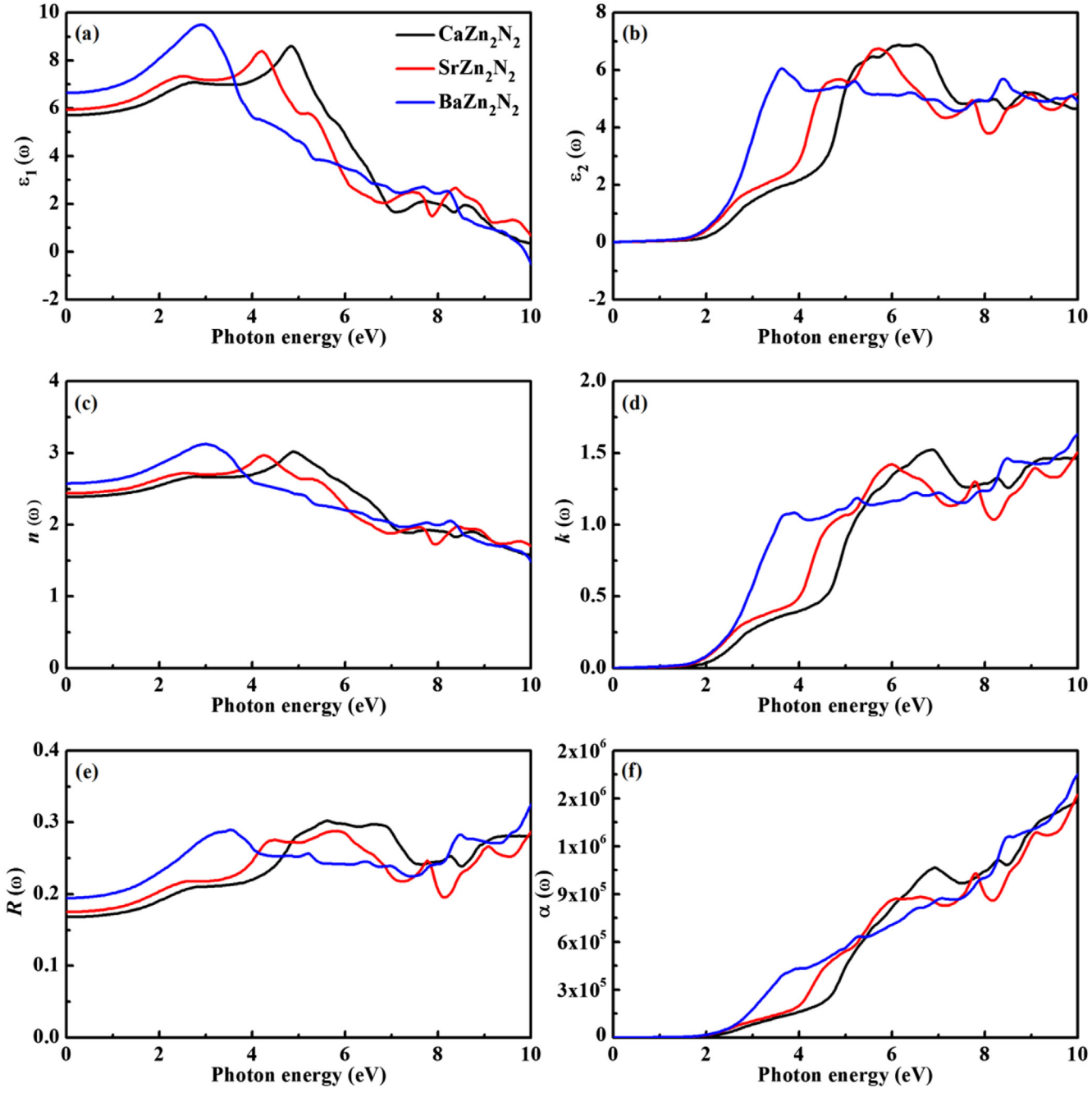

Fig. 7 The optical properties of AZn_2N_2 (A = Ca, Sr, Ba): (a) $\varepsilon_1(\omega)$, (b) $\varepsilon_2(\omega)$, (c) $n(\omega)$, (d) $k(\omega)$, (e) $R(\omega)$, and (f) $\alpha(\omega)$.

the effective masses of electron and hole are in the range of 0.2–0.3 m_0 and 1.3–1.4 m_0, respectively. There is an inverse relationship between the effective mass and conductivity (Khan et al., 2021), so the electron shows better mobility for carrier transport. The value of E_b varies between 60 and 80 meV, which indicates that each compound is suitable for application as an absorption layer in solar cells.

3.4. Optical properties

The light harvesting capacity of a semiconductor material is a crucial index for photovoltaic applications. The various optical properties are directly related to the dielectric function $\varepsilon(\omega)$, which is given as follows (Tang et al., 2019):

$$\varepsilon(\omega) = \varepsilon_1(\omega) + i\varepsilon_2(\omega) \tag{5}$$

where $\varepsilon_1(\omega)$ and $\varepsilon_2(\omega)$ represent the real part and imaginary part of the dielectric function, respectively. The calculated curves of $\varepsilon_1(\omega)$ and $\varepsilon_2(\omega)$ are shown in Fig. 7(a-b). The values of static dielectric constants $\varepsilon_1(0)$ are 5.70, 5.94, and 6.64 for $CaZn_2N_2$, $SrZn_2N_2$, and $BaZn_2N_2$, respectively. The $\varepsilon_2(\omega)$ peak of $BaZn_2N_2$ is higher than those of $CaZn_2N_2$ and $SrZn_2N_2$ in the photon energy range from 2 to 5 eV, indicating that $BaZn_2N_2$ has better absorption capacity for visible light.

In addition, the refractive index $n(\omega)$, extinction coefficient $k(\omega)$, reflectivity $R(\omega)$, and absorption coefficient $\alpha(\omega)$ of $CaZn_2N_2$, $SrZn_2N_2$, and $BaZn_2N_2$ are computed by the following relations (Zhao et al., 2021):

$$n(\omega) = [\frac{\varepsilon_1(\omega)}{2} + \frac{\sqrt{\varepsilon_1^2(\omega) + \varepsilon_2^2(\omega)}}{2}]^{\frac{1}{2}} \quad (6)$$

$$k(\omega) = [\frac{-\varepsilon_1(\omega)}{2} + \frac{\sqrt{\varepsilon_1^2(\omega) + \varepsilon_2^2(\omega)}}{2}]^{\frac{1}{2}} \quad (7)$$

$$R(\omega) = \frac{[n(\omega) - 1]^2 + k^2(\omega)}{[n(\omega) + 1]^2 + k^2(\omega)} \quad (8)$$

$$\alpha(\omega) = \sqrt{2}\omega\left[\sqrt{\varepsilon_1(\omega)^2 + \varepsilon_2(\omega)^2} - \varepsilon_1(\omega)\right]^{1/2} \quad (9)$$

The calculated results are plotted in Fig. 7(c-f). It can be seen that the curves of $n(\omega)$ and $k(\omega)$ are similar to those of $\varepsilon_1(\omega)$ and $\varepsilon_2(\omega)$. The static value of refractive index $n(0)$ can be obtained by the equation $n(0) = \sqrt{\varepsilon_1(0)}$ (Li et al., 2008). The calculated $n(0)$ values are 2.39, 2.44, and 2.58 for $CaZn_2N_2$, $SrZn_2N_2$, and $BaZn_2N_2$, respectively. The static value of $k(0)$ is close to zero in the low photon energy region (0–2 eV). The static values of $R(0)$ are 0.168 for $CaZn_2N_2$, 0.175 for $SrZn_2N_2$, and 0.194 for $BaZn_2N_2$, respectively. The value of $R(\omega)$ always fluctuates between 0.15 and 0.35 in the range of 0–10 eV. It is observed from Fig. 7(f) that the absorption edge is mostly located at about 2 eV, which is linked with the band gap calculated by the direct electronic transition from the top of the valence band to the bottom of the conduction band. In the low photon energy range (0–2 eV), the absorption is negligible. Three compounds show the high light absorption properties. Especially, the efficiency of light absorption is greatly enhanced for $BaZn_2N_2$ in the visible and ultraviolet regions (2–5 eV), which is very conducive to improve the optical performance.

4. Conclusions

In summary, the structure, stability, elastic, electronic, and optical properties of trigonal AZn_2N_2 (A = Ca, Sr, Ba) are revealed for the first time in the current work. The stability and optoelectronic properties of $BaZn_2N_2$ are highlighted. The results show that three compounds are thermodynamically and mechanically stable, and they are brittle materials. Moreover, the stability of $BaZn_2N_2$ is further verified by applying different theoretical approaches. The direct band gap transition at the Γ point is allowed for each compound. The calculated direct band gaps are 1.733, 1.507, and 1.510 eV for $CaZn_2N_2$, $SrZn_2N_2$, and $BaZn_2N_2$, respectively. For three compounds, the electron exhibits high mobility for carrier transport, and the value of E_b is less than 80 meV. Detailed analysis of optical properties displays that $BaZn_2N_2$ has excellent light absorption capacity in the visible region. This findings reveal that $BaZn_2N_2$ is a good candidate for optoelectronic applications.

CRediT authorship contribution statement

Diwen Liu: Conceptualization, Supervision, Validation, Writing – original draft. **Huan Peng:** Formal analysis. **Rongjian Sa:** Resources, Writing – review & editing.

Declaration of competing interest

The authors declare that they have no known competing financial interests or personal relationships that could have appeared to influence the work reported in this paper.

Acknowledgments

This work was supported by the Science and Technology Research Program of the Education Department of Jiangxi Province (No. GJJ212705).

References

Blöchl, P.E., 1994. Projector augmented-wave method. Phys. Rev. B 50, 17953–17979.
Cao, X., Kawamura, F., Ninomiya, Y., Taniguchi, T., Yamada, N., 2017. Conduction-band effective mass and bandgap of $ZnSnN_2$ earth-abundant solar absorber. Sci. Rep. 7, 14987.
Green, M.A., 1990. Intrinsic concentration, effective densities of states, and effective mass in silicon. J. Appl. Phys. 67, 2944–2954.
Hadi, M.A., Roknuzzaman, M., Chroneos, A., Naqib, S.H., Islam, A. K.M.A., Vovk, R.V., Ostrikov, K., 2017. Elastic and thermodynamic properties of new $(Zr_{3-x}Ti_x)AlC_2$ MAX-phase solid solutions. Comput. Mater. Sci. 137, 318–326.
Häusler, J., Schimmel, S., Wellmann, P., Schnick, W., 2017. Ammonothermal Synthesis of Earth-Abundant Nitride Semiconductors $ZnSiN_2$ and $ZnGeN_2$ and Dissolution Monitoring by In Situ X-ray Imaging. Chem. Eur. J. 23, 12275–12282.
Häusler, J., Niklaus, R., Minár, J., Schnick, W., 2018. Ammonothermal Synthesis and Optical Properties of Ternary Nitride Semiconductors Mg-IV-N_2, Mn-IV-N_2 and Li-IV_2-N_3 (IV = Si, Ge). Chem. Eur. J. 24, 1686–1693.
Heyd, J., Scuseria, G.E., Ernzerhof, M., 2003. Hybrid functionals based on a screened Coulomb potential. J. Chem. Phys. 118, 8207–8215.
Hill, R., 1952. The Elastic Behaviour of a Crystalline Aggregate. Proc. Phys. Soc. Sect. A 65, 349–354.
Hinuma, Y., Hatakeyama, T., Kumagai, Y., Burton, L.A., Sato, H., Muraba, Y., Iimura, S., Hiramatsu, H., Tanaka, I., Hosono, H., Oba, F., 2016. Discovery of earth-abundant nitride semiconductors by computational screening and high-pressure synthesis. Nat. Commun. 7, 11962.
Huang, M., Wang, S., Zhang, T., Chen, S., 2022. Searching for Band-Dispersive and Defect-Tolerant Semiconductors from Element Substitution in Topological Materials. J. Am. Chem. Soc. 144, 4685–4694.
Khan, A.A., Rehman, A.U., Laref, A., Yousaf, M., Murtaza, G., 2018. Structural, Optoelectronic and Thermoelectric Properties of Ternary $CaBe_2X_2$ (X = N, P, As, Sb, Bi) Compounds. Z. Naturforsch. A 73, 965–973.
Khan, A.A., Yaseen, M., Laref, A., Murtaza, G., 2018. Impact of anion replacement on the optoelectronic and thermoelectric properties of $CaMg_2X_2$, X = (N, P, As, Sb, Bi) compounds. Phys. B Condens. Matter 541, 24–31.
Khan, A.A., Hasil, R., Laref, A., Ullah, N., Sajjad, M., Zeb, A., Murtaza, G., 2019. DFT prediction of the structural, electronic, thermoelectric and optical properties of ternary pnictides $MgBe_2X_2$ (X = N, P, As, Sb, Bi): A novel analysis of beryllium with 2A- and 5B-Elements of the structure type $CaAl_2Si_2$. Solid State Commun. 300, 113667.
Khan, I., Shahab, I.U., Haq, A., Ali, Z., Ali, I., 2021. Ahmad, Elastic and Optoelectronic Properties of Cs_2NaMCl_6 (M = In, Tl, Sb, Bi). J. Electron. Mater. 50, 456–466.

Kikuchi, R., Ueno, K., Nakamura, T., Kurabuchi, T., Kaneko, Y., Kumagai, Y., Oba, F., 2021. $SrZn_2N_2$ as a Solar Absorber: Theoretical Defect Chemistry and Synthesis by Metal Alloy Nitridation. Chem. Mater. 33, 2864–2870.

Kresse, G., Furthmüller, J., 1996. Efficiency of ab-initio total energy calculations for metals and semiconductors using a plane-wave basis set. Comput. Mater. Sci. 6, 15–50.

Laidouci, A., Aissat, A., Vilcot, J.P., 2020. Numerical study of solar cells based on $ZnSnN_2$ structure. Sol. Energy 211, 237–243.

Li, C., Lu, X., Ding, W., Feng, L., Gao, Y., Guo, Z., 2008. Formability of ABX_3 (X = F, Cl, Br, I) halide perovskites. Acta Cryst. B 64, 702–707.

Liu, D., Peng, H., Huang, J., Sa, R., 2022. Revealing the stability and optoelectronic properties of novel nitride and phosphide semiconductors: A DFT prediction. Surf. Interfaces 29, 101740.

Liu, Y., Wang, W., Xiao, F., Xiong, L., Ming, X., 2021. Stability and optoelectronic property of lead-free halide double perovskite Cs_2-B'BiI_6 (B' = Li, Na and K). Chin. Phys. B 30, 108102.

Mallmann, M., Niklaus, R., Rackl, T., Benz, M., Chau, T.G., Johrendt, D., Minár, J., Schnick, W., 2019. Solid Solutions of Grimm-Sommerfeld Analogous Nitride Semiconductors II-IV-N_2 (II = Mg, Mn, Zn; IV = Si, Ge): Ammonothermal Synthesis and DFT Calculations. Chem. Eur. J. 25, 15887–15895.

Meng, W., Wang, X., Xiao, Z., Wang, J., Mitzi, D.B., Yan, Y., 2017. Parity-Forbidden Transitions and Their Impact on the Optical Absorption Properties of Lead-Free Metal Halide Perovskites and Double Perovskites. J. Phys. Chem. Lett. 8, 2999–3007.

Mouhat, F., Coudert, F.-X., 2014. Necessary and sufficient elastic stability conditions in various crystal systems. Phys. Rev. B 90, 224104.

Murtaza, G., Ahad Khan, A., Yaseen, M., Laref, A., Ullah, N., Ur Rahman, I., 2018. The effect of replacing pnictogen elements on the physical properties $SrMg_2X_2$ (X = N, P, As, Sb, Bi) Zintl compounds. Chin. Phys. B 27.

Murtaza, G., Yousaf, N., Laref, A., Yaseen, M., 2018. Effect of Varying Pnictogen Elements (Pn = N, P, As, Sb, Bi) on the Optoelectronic Properties of $SrZn_2Pn_2$. Z. Naturforsch. A 73, 285–293.

Murtaza, G., Yousaf, N., Yaseen, M., Laref, A., Azam, S., 2018. Systematic studies of the structural and optoelectronic characteristics of $CaZn_2X_2$ (X = N, P, As, Sb, Bi). Mater. Res. Express 5, 016304.

Özdemir, U., Korcak, S., Gültekin, A., Öztürk, M.K., 2019. Investigation of structural, electronic, elastic, optical and dynamical properties of $Ga_{1-x}Al_xN$ alloys. Mater. Res. Express 6, 096318.

Perdew, J.P., Burke, K., Ernzerhof, M., 1996. Generalized Gradient Approximation Made Simple. Phys. Rev. Lett. 77, 3865–3868.

Pugh, S.F., 1954. XCII. Relations between the elastic moduli and the plastic properties of polycrystalline pure metals. Lond. Edinburgh Dublin Philos. Magaz. J. Sci. 45, 823–843.

Tang, Y., Zhang, J., Zhong, X., Wang, Q., Zhang, H., Ren, C., Wang, J., 2019. Revealing the structural, electronic and optical properties of lead-free perovskite derivatives of Rb_2SnX_6(X = Cl, Br and I): A theory calculation. Sol. Energy 190, 272–277.

Togo, A., Tanaka, I., 2015. First principles phonon calculations in materials science. Scr. Mater. 108, 1–5.

Tsuji, M., Hanzawa, K., Kinjo, H., Hiramatsu, H., Hosono, H., 2019. Heteroepitaxial Thin-Film Growth of a Ternary Nitride Semiconductor $CaZn_2N_2$. ACS Appl. Electron. Mater. 1, 1433–1438.

Tsuji, M., Hiramatsu, H., Hosono, H., 2019. Tunable Light Emission through the Range 1.8–3.2 eV and p-Type Conductivity at Room Temperature for Nitride Semiconductors, $Ca(Mg_{1-x}Zn_x)_2N_2$ (x = 0–1). Inorg. Chem. 58, 12311–12316.

Tsunoda, N., Kumagai, Y., Takahashi, A., Oba, F., 2018. Electrically Benign Defect Behavior in Zinc Tin Nitride Revealed from First Principles. Phys. Rev. Appl. 10, 011001.

Ul Haq, B., Ahmed, R., Shaari, A., El Haj Hassan, F., Kanoun, M.B., Goumri-Said, S., 2014. Study of wurtzite and zincblende GaN/InN based solar cells alloys: First-principles investigation within the improved modified Becke-Johnson potential. Sol. Energy 107, 543–552.

Wines, D., Ersan, F., Ataca, C., 2020. Engineering the Electronic, Thermoelectric, and Excitonic Properties of Two-Dimensional Group-III Nitrides through Alloying for Optoelectronic Devices ($B_{1-x}Al_xN$, $Al_{1-x}Ga_xN$, and $Ga_{1-x}In_xN$). ACS Appl. Mater. Interfaces 12, 46416–46428.

Wu, Z.-J., Zhao, E.-J., Xiang, H.-P., Hao, X.-F., Liu, X.-J., Meng, J., 2007. Crystal structures and elastic properties of superhard Ir_2 and IrN_3 from first principles. Phys. Rev. B 76, 054115.

Yamada, N., Mizutani, M., Matsuura, K., Imura, M., Murata, H., Jia, J., Kawamura, F., 2021. Band Gap-Tunable (Mg, Zn)SnN_2 Earth-Abundant Alloys with a Wurtzite Structure. ACS Appl. Electron. Mater. 3, 4934–4942.

Zhao, Y.-Q., Hu, C.-E., Liu, L., Cheng, Y., Cai, L.-C., 2017. First-Principles Investigations on Structural, Elastic, Dynamical, and Thermal Properties of Earth-Abundant Nitride Semiconductor $CaZn_2N_2$ under Pressure. Z. Naturforsch. A 72, 39–49.

Zhao, X.-H., Wei, X.-N., Tang, T.-Y., Gao, L.-K., Xie, Q., Lu, L.-M., Tang, Y.-L., 2021. First-principles study on the structural, electronic and optical properties of vacancy-ordered double perovskites Cs_2PtI_6 and Rb_2PtI_6. Opt. Mater. 114, 110952.